Evidence for different regimes of collective flux-line pinning in $YBa_2Cu_3O_{7-\delta}$ single crystals

R. Hiergeist and R. Hergt
Institut für Physikalische Hochtechnologie e.V. Jena, PF 100239, D-07702 Jena, Germany
(Received 18 July 1996; revised manuscript received 7 October 1996)

$YBa_2Cu_3O_{7-\delta}$ single crystals with different microstructure of the twin pattern were studied by means of torque magnetometry. Current densities and pinning force volume densities were calculated from torque hysteresis data. Pinning force volume density F_p in dependence on the component B_z of the flux density parallel to the c-axis direction revealed different regimes of collective pinning: For very low B_z, in the single vortex pinning regime, current density is independent on B_z. With increasing B_z a transition towards the regime of collective pinning of small flux bundles occurs. Here two different cases can be distinguished. For pinning at randomly distributed point pinning centers a strong influence of thermal oscillations of flux lines within the pinning barriers can be observed. In contrast, for single crystals having a ''mosaic'' twin structure, the influence of thermal oscillations can be neglected due to a fraction of flux lines which are strongly correlated pinned by twin planes and hinder the thermal oscillations of the other weakly pinned flux lines in the flux bundles. In both cases an increase of the current density with increasing B_z (i.e., ''fishtail'' effect) can be observed, which is characterized, at low B_z, by a power-law behavior $F_p \sim B_z^p$ with $p=7/4$ for collective random point pinning of small flux bundles and $p=2$ for pinning of small flux bundles with additional correlated pinning contributions from the mosaic twin structures, respectively. For $YBa_2Cu_3O_{7-\delta}$ single crystals, with only medium current density but with a mosaic twin structure, a ''lock-in'' transition from pure collective random point pinning of large flux bundles, which is strongly influenced by thermal oscillations, towards collective pinning of small bundles with contributions of correlated pinning can be observed. [S0163-1829(97)08805-X]

I. INTRODUCTION

The theory of collective pinning of flux lines by randomly distributed weak point pinning centers of high number density was established by Larkin and Ovchinnikov[1] (LO) in 1973, many years before the new cuprate high-T_c (HTS) materials were discovered. Good scaling of experimental data of pinning force volume density as a function of the perpendicular magnetic field with the LO theory was reported first time by Kes and Tsuei[2] for amorphous Nb_3Ge films. But above a certain limiting value of B the pinning force volume density grows much faster than predicted by the 2D collective pinning theory. This so-called ''peak'' effect could be observed for many low-temperature superconductors (LTS) as a peak in the current density j with increasing external magnetic field at fields close to the upper critical field B_{c2}. According to Kes and Tsuei[2] the ''peak'' effect in thin amorphous Nb_3Ge films is caused by increased pinning mediated disorder, i.e., by defects in the flux-line lattice (FLL). Due to lowered shear modulus close to B_{c2} FLL is plastically deformed and a better adaptation of the flux lines to the pinning centers will be achieved. Larkin and Ovchinnikov[1] gave an explanation in terms of a softening of the FLL due to the strong dispersion of the tilt modulus $c_{44}(\mathbf{q})$ close to H_{c2}. Sugawara *et al.*[3] found for layered superconductors that this model is able to describe the ''peak'' effect quantitatively. Nevertheless, they found that some discrepancies between the experimental data and the theory remain unsolved. In the case of thick amorphous films a first-order phase transition due to a dimensional crossover from 2D collective pinning towards 3D pinning was discussed by Wördenweber and Kes[4] as a reason for an observed jump in the pinning force volume density $F_p(B)$.

In order to extend the concept of collective pinning to HTS materials Feigel'man and Vinokur[5] included thermal oscillations of flux lines in the LO theory: At high temperatures current densities may be strongly reduced due to the influence of thermal fluctuations on pinning properties not only by thermally activated jumps between different metastable states of the flux-line lattice which leads to significant flux-creep effects, but also by thermal fluctuations of the flux lines within the pinning barriers which smear out the elementary pinning potential. In the case of the new class of high-T_c superconductors we deal with extreme type-II superconductors with properties which favor the occurrence of collective pinning. The short coherence length in the ab direction, ξ_{ab}, the modulation of the order parameter in the c-axis direction, and the low density of charge carriers are the reasons that elementary pinning energies are so small in HTS and that a high density of point defects in the superconducting ab planes can act as a dense array of pinning centers with low pinning energy. Large penetration depths, on the other hand, enable strong elastic vortex interactions.

Experimentally, an increase of the magnetization hysteresis with increasing external magnetic field is often observed in magnetization measurements of $YBa_2Cu_3O_{7-\delta}$ single crystals for field orientation parallel to the c-axis direction and magnetic fields far below H_{c2}.[6] To explain this so-called ''fishtail'' effect different competing models were proposed which are in most cases similar to those models which were developed in order to explain the ''peak'' effect in LTS materials. One class of models is based on the assumption of microstructural inhomogeneities (e.g., Refs. 6 and 7). It is supposed that small regions with lower H_{c2} than the sur-

rounding $YBa_2Cu_3O_7$ matrix, for instance, regions with low oxygen content, will switch after exceeding their upper critical field into the normal state and therefore work as additional pinning centers.[6] In another quite similar model, these regions with low oxygen content act as weak pinning centers at low magnetic fields, but will have an enhanced pinning force at higher magnetic fields. However, this hypothesis could not be confirmed by more careful experimental work (e.g., Ref. 8). The peak field $H_{\rm peak}$, which may be identical with H_{c2} of the switching region, varies much slower with temperature than H_{c2} (T) of $YBa_2Cu_3O_{7-\delta}$ single crystals with low oxygen content.[7] In particular, Zhukov *et al.*[9] found that the common ''fishtail'' is present for all oxygen contents up to fully oxygenated $YBa_2Cu_3O_{7-\delta}$ single crystals ($\delta < 0.02$) even at temperatures close to T_c. Differences in the dependence of the superconducting order parameter on magnetic field between possible weak superconducting regions and the surrounding matrix seem to be too small to explain the pronounced magnetization peak, which can be observed especially at temperatures in the range between 70 and 80 K. Therefore an enhancement of the elementary pinning interaction due to the magnetic field seems not to be very reasonable.

A second category of models tries to give an explanation on the basis of relaxational effects (e.g., Refs. 10–12). In the approach suggested by Krusin-Elbaum *et al.*[12] the ''fishtail'' effect is caused by the discrepancy between critical current density j_c, which is defined by the current density when the effective pinning potential U vanishes, i.e., by $U(j_c)=0$, and the current density measured in experiment. The current density in experiment is not sharply defined. It depends on the voltage criterion, i.e., on the strength of the applied electric field, and is lower than j_c because experiments are usually made in the nonlinear region of current voltage characteristics. According to Krusin-Elbaum *et al.*[12] the ''fishtail'' effect is caused by a higher flux creep rate for lower flux density leading to a depression of the measured current density. They explain the change of the creep rate by a transition from individually pinned flux lines to the pinning of small flux bundles. Implicitly this model requires that the critical current density does not depend in the same nonmonotonous way on flux density as the experimentally measured ''fishtail'' current density does. However, the reported ''mirror-like'' behavior of current density and creep rate could not be confirmed by measurements with better field resolution in the low-field region of the current peak.[13] Küpfer *et al.*[14] found similar creeprates for different samples of YBCO material regardless whether magnetic hysteresis was monotonous decreasing with increasing field, i.e., ''fishtail'' behavior was observed. From this result they concluded that the ''fishtail'' effect cannot be explained by different field-dependent regimes of collective flux creep.

A ''peak'' effect in $YBa_2Cu_3O_{7-\delta}$ single crystals was reported by Kwok *et al.*[15] as a precursor to vortex lattice melting. A model was proposed by Larkin, Marchetti, and Vinokur[16] which ascribes this effect to a softening of the shear modulus c_{66} close to the melting line $T_m(B)$, which abruptly lowers the argument in the exponentially decreasing term of the current density in the regime of small flux line bundles.

It should be mentioned that there are as well several other models for the explanation of anomalous field dependences which use other concepts like dimensional crossover, surface barriers, or matching effects in order to explain an increased pinning. As we will show in this paper the ''fishtail'' effect in $YBa_2Cu_3O_{7-\delta}$ single crystal samples may be understood in terms of a hardening of the flux-line lattice in the regime of collective pinning of small flux bundles for low B. In Sec. II we will discuss important consequences from the collective pinning theory[5] in order to provide the basis for an understanding of the experimental results and the data evaluation in terms of the collective pinning theory. Samples and experimental method will be described in Sec. III. The experimental results will be discussed in relation to the different microstructure of the crystals and different pinning regimes will be identified in Sec. IV. A transition from single vortex pinning to small bundle pinning for the case of randomly distributed point pinning centers is found. Although the case of correlated pinning is not included in the original collective pinning theory of Feigel'man and Vinokur,[5] we discuss the effect of additional contributions of correlated pinning due to twin mosaic structure. According to these two types of defect structures two different power laws for the ''fishtail'' effect are found. A quantitative explanation in terms of the collective pinning theory[5] is provided.

II. CURRENT DENSITIES FOR CHARACTERISTIC PINNING REGIMES

According to Larkin and Ovchinnikov[1] pinning of flux lines at weak, randomly distributed point pinning centers of high concentration destroys the long-range order of the flux-line lattice. But within a volume V_c, the ''correlation volume,'' short-range order of the FLL with an almost periodical structure still persists. For an Abrikosov 3D vortex lattice the elastic contribution to the free energy of the FLL can be described in terms of the compression modulus c_{11}, the shear modulus c_{66}, and the tilt modulus c_{44}. Because c_{11} is much larger than c_{66} and c_{44}, contribution of compression to elastic energy is small and terms containing c_{11} can be neglected.[1,5] For c_{66} and c_{44} one can write for temperatures and flux densities below the melting line[1,17]

$$c_{66}=\frac{\Phi_0 B}{16\pi\mu_0\lambda^2}, \quad c_{44}(q)=\frac{B^2}{\mu_0}\frac{1}{(q\lambda)^2+1}, \tag{1}$$

where λ is the London penetration depth, Φ_0 is the flux quantum and $\mathbf{q}$ the wave vector of the reciprocal space representation of the transversal displacement field $\mathbf{u}(\mathbf{r})$, which is due to the random point pinning of the distorted FLL. For very weak pinning or very high flux densities the volume of short-range order spreads out over a large fraction of the FLL and therefore correlation volume is large. Flux lines within the correlation volume are not pinned individually but collectively as one ''flux bundle.'' For stronger pinning or lower flux density the size of the flux bundle decreases. If the lateral dimension R_c of the correlation volume $V_c \approx R_c^2 L_c$ is becoming much smaller than $\lambda_\perp$, the penetration depth perpendicular to the vortex direction, a transition from collective pinning of ''large flux bundles'' towards collective pinning of ''small flux bundles'' is taking place. The latter one is characterized by a large dispersion[5] ($q\lambda \gg 1$) of the tilt modulus $c_{44}(\mathbf{q}) \simeq B^2/[\mu_0(q\lambda)^2]$ whereas dispersion can be

neglected in the former case ($q\lambda \ll 1$) and $c_{44}(\mathbf{q}) = c_{44}(0) \simeq B^2/\mu_0$. If pinning is further increased or if flux density is further decreased even short scale order of the flux-line lattice will be destroyed: Elastic interactions between flux lines can be neglected in comparison to the contributions of the elementary pinning barriers. In this so-called ''single vortex pinning'' regime all vortices are pinned individually.

Besides the disorder due to random point pinning there is also a thermally induced disorder. According to Feigel'man and Vinokur[5] there is a significant influence of thermal fluctuations of flux lines within the pinning barriers for a weakly pinned FLL if the mean-square thermal displacement of flux lines $\langle u^2 \rangle$ in an unpinned FLL is of the same order or even larger than the square of the range of the pinning barriers, i.e., if $\langle u^2 \rangle \geqslant \xi^2$. This is true for temperatures higher than the so-called ''depinning temperature'' which was estimated to[5,18]

$$T_L^*(B) = \frac{\epsilon \Phi_0^{3/2}}{\mu_0 k_B \pi \kappa^2} \sqrt{B}, \tag{2}$$

where $\epsilon^2 = m_{ab}/m_c$ denotes the anisotropy ratio of the effective electron masses for electrons moving in ab direction and c-axis direction, respectively.

Characteristic current densities near to criticality were estimated by Feigel'man and Vinokur[5] by solving perturbatively differential equations which describe transverse FLL motion for the different isotropic collective pinning regimes under the influence of thermal Langevin forces. In the ''single vortex pinning'' regime the current density is independent on flux density $j_{sv} = \text{const}$. For collective pinning of small flux bundles, i.e., for higher flux density, a significant influence of the flux density on the current density is expected according to Ref. 5:

$$j_{sb} = \frac{3\sqrt{3}}{32\pi} j_0 \frac{B}{B_{c2}} \left(1 + \frac{T}{T_L^*}\right)^{1/2} \times \exp\left[-\pi\sqrt{2}\left(\frac{B}{B_{c2}}\right)^{3/2} \frac{\gamma_{\max}}{\gamma}\left(1 + \frac{T}{T_L^*}\right)^3\right], \tag{3}$$

where $j_0 = \Phi_0/(3\sqrt{3}\mu_0 \pi \lambda^2 \xi)$ denotes the depairing current density and B_{c2} the upper critical flux density. Thermal fluctuations of flux lines are taken into account by T/T_L^*. The correlation properties of neighboring defects are considered by the parameter γ (cf. Ref. 5). $\gamma_{\max}$ denotes the value of γ in the limit of maximum correlation of pinning centers, i.e., for a distance between neighboring pinning centers in the order of ξ. Considering the expressions of Eq. (1) and the relations $B_c^2 = \Phi_0 B_{c2}/(4\pi\lambda^2)$ and $\gamma_{\max}/\gamma = (j_0/j_{sv})^{3/2}/4\pi$, Eq. (3) can be written in the form[16]

$$j_{sb} = \frac{3\mu_0\sqrt{3}}{8\pi B_c^2} j_0 c_{66} \left(1 + \frac{T}{T_L^*}\right)^{1/2} \exp\left[-\left(\frac{j_0}{j_{sv}}\frac{\mu_0}{B_c^2}\right)^{3/2} \times \frac{8\sqrt{2\mu_0}}{B} c_{44}(0)^{1/2} c_{66}^{3/2} \left(1 + \frac{T}{T_L^*}\right)^3\right]. \tag{4}$$

For even higher flux densities or lower current density ($j \ll j_0/\kappa^2$) a transition towards large flux bundles will occur, with the characteristic current density

$$j_{lb} \cong 10 \frac{j_0}{\kappa^2} \left(\frac{\gamma}{\gamma_{\max}}\right)^2 \left(\frac{B_{c2}}{B}\right)^3 \left(1 + \frac{T}{T_L^*}\right)^{-11/2}. \tag{5}$$

The transition line from single vortex pinning towards collective pinning not only depends on flux density and temperature but also on current density (cf. Ref. 19, p. 1152), i.e., on the voltage criterion. The crossover from pinning of individual flux lines, at low flux densities, towards collective pinning of flux bundles can be roughly estimated by comparing the interaction energy, i.e., the elastic shear energy, with the tilt energy of an individual flux line (cf. Ref. 19, p. 1167). Line tension is strongly reduced in HTS materials due to the suppression of the order parameter between the superconducting layers. In addition the thermal fluctuations of the flux lines have to be taken into account for the determination of the transition lines between the different regimes. In general, with increasing current density the regime of single vortex pinning will be extended to higher fields (cf. Ref. 19, p. 1152).

Many attempts have been made in the literature to analyse experimental flux-creep data by identifying the characteristic parameters μ of the different regimes of collective flux creep in terms of the so-called interpolation formula[5] for the activation energy $U(j) = (U_c/\mu)[(j_c/j)^\mu - 1]$. Since in most cases magnetic measurements are starting from high voltage criterion, i.e., from currents near criticality, the contribution of compression energy has to be considered in addition to the activation energy. This leads, at high flux densities, to a theory of collective hopping of superbundles (cf. Ref. 19, p. 1208), which consist of many flux bundles. In this case flux creep can be described by a slightly different formula $U(j) = U_c(1 - j/j_c)^\alpha$. Unfortunately the exponents α for creep of superbundles in random pinning potential are still unknown (cf. Ref. 19, p. 1210). Deviation from the interpolation formula may also be due to high temperatures $T \gg T_L^*$, since the interpolation formula is only valid in the regime below the depinning line $T_L^*(B)$ (cf. Ref. 5). From the influence of current density on the predominance of the different collective pinning regimes it follows that in general it is difficult to get useful conclusions concerning collective pinning from the analysis of flux-creep experiments: With decreasing j different collective pinning regimes can be passed. From the same reason practicability of back extrapolation[20] onto the ''true'' critical current density from data of creep experiments or magnetic sweep measurements with different sweep rates is limited.

The temperature dependence of experimental current density at fixed field was already discussed by Moshchalkov, Metlushko, and Güntherodt[21,22] for $Bi_2Sr_2CaCu_2O_x$ single crystals in the framework of the collective pinning theory. In the present paper we will analyse the field dependence of experimental $j(B)$ curves in the framework of the predicted $j(B)$ dependences of Eqs. (3)–(5) for fixed temperature. Therefore the complicated temperature dependence of the characteristic current densities arising from the temperature dependence of the different parameters like depairing current density j_0 or B_{c2} in Eqs. (3)–(5) can be omitted.

In the following we will discuss experimental results on $YBa_2Cu_3O_{7-\delta}$ single crystals with different microstructure in terms of Eqs. (2)–(5). It will be demonstrated that the pin-

TABLE I. Crystal properties.

Sample	T_c (K)	ΔT_c (K)	s (μm)
A	90	1	1.3
B	89	2	~1
C	91	0.5	<0.3
D	90	0.2	0.8

ning behavior of $YBa_2Cu_3O_{7-\delta}$ single crystals can be understood within the framework of the collective pinning theory.

III. EXPERIMENTAL DETAILS

A. Sample preparation and characteristics

The present experiments were performed on $YBa_2Cu_3O_{7-\delta}$ single crystals which were grown in yttrium stabilized ZrO crucibles according to a procedure described in detail elsewhere.[23,24] Crystals were grown in different batches using identical experimental conditions. For standard annealing conditions (1 week at 400 °C at 0.1 MPa oxygen pressure) ac-susceptibility measurements[25] showed that the transition temperature to the normal state is always $T_c \geqslant 90$ K with transition width of about $\Delta T_c = 0.2,\ldots,2$ K. The microstructure of the twin pattern of the samples was characterized by polarization microscopy. Four samples with representative behavior were selected for detailed measurements. The first sample *A* contains only one set of parallel twin planes. Samples *C* and *D* contain a mosaic pattern which is formed by two sets of twin planes being oriented perpendicularly to each other. Additionally we take into account the sample *B* annealed under enhanced oxygen pressure of 200 bar at 380 °C. This crystal also shows a mosaic twin pattern. The mosaic pattern seen in polarized light is known in the literature as fuzzy domains. By analyzing that pattern we have estimated the average twin spacing which is denoted by s. Characteristic data of the samples are given in Table I. The crystals are free of macroscopic defects or precipitations. By TEM investigations[26] no defects on a scale above about 3 nm were found.

However, from the observed current densities which are very high (up to 200 kA/cm^2) in comparison to what is commonly known for single crystals we expect that there are many effective pinning centers on an atomic scale. The most prominent candidates for those pinning centers are oxygen vacancies as argued currently in literature.[6] According to Claus *et al.*[24] there is a maximum of T_c for a weak deviation from oxygen stoichiometry. Comparing our crystals *A*, *B*, and *C* with the data of the samples of Ref. 24 which were got by a similar growth procedure as applied in the present investigations we conclude that we deal with an oxygen nonstoichiometry of $\delta = 0.15$. Another possible candidate for point pinning centers are impurities from dissolved crucible material which were incorporated into crystals during the growth process and may produce point defects of atomic scale.

B. Torque magnetometry with rotating external magnetic field

Torque measurements with rotating external magnetic field were performed at constant temperature of 77.4 K after zero-field cooling. The procedure was described in detail recently.[27] For field strength up to 0.8 T, a constant field was turned in a plane which contains the c axis. The torque G exerted on the sample was measured in dependence on the angle between field direction and the c axis. Measurements were carried out for field rotation with forward (G_f) and reverse rotational sense (G_r) which yield the torque hysteresis ΔG:

$$\Delta G = G_f - G_r . \tag{6}$$

In all torque measurements with rotating external field, a fixed voltage criterion for the case of external magnetic field parallel to the ab planes ($\vartheta_H \cong \theta = 90°$) was achieved by keeping the product of angular velocity ω of our rotating field and the value of the external field constant. We used always the same value of the voltage criterion for this field orientation of $E \approx 2.5 \times 10^{-6}$ V/m in all of our measurements. Therefore the field rotation rate was chosen appropriately with an accuracy of 2.5% in order to control the induced electric field

$$E \approx \frac{d}{2}\,\mu_0 \left[\frac{dH_z}{dt} + (1 - N_{zz})\,\frac{dM_z}{dt} \right] \approx \frac{d}{2}\,\mu_0\,\frac{dH_z}{dt}. \tag{7}$$

Here d denotes the width of the sample in the ab plane, H_z the component of the external magnetic field **H** parallel to the c axis, N_{zz} the zz component of the demagnetization tensor for the z direction parallel to the c axis and M_z the component of the magnetization parallel to the c-axis direction.[27] Because of the high aspect ratios of the samples with dimensions of 0.15, . . . ,0.35 mm in the c-axis direction and 0.5, . . . ,2.2 mm lateral size the contribution of dM_z/dt can be neglected in first order because of the high values of $N_{zz} \approx 1$.

In principle, in a field rotation experiment a deviation of the angular orientations of the external magnetic field and the flux density occurs. Due to the constant amount of the external magnetic field during the rotations, which was always much higher than the lower critical field in the c-axis direction H_{c1}^c, deviations of the angular orientation θ of flux lines with respect to the c-axis direction from ϑ_H the angular orientation of the external magnetic field with respect to the c-axis direction are very small. Corrections carried out on the experimental data showed no significant angular deviation except for very low external field strength and field orientation close to the ab planes.

The angular dependence of the torque hysteresis ΔG measured for stationary rotation of the external magnetic field H was used to derive the irreversible part of the magnetization $M_{\rm irr}$, and the current density j according to

$$M_{\rm irr} = \Delta G / (\mu_0 H V \sin\vartheta_H), \tag{8}$$

$$j = k M_{\rm irr} / d, \tag{9}$$

where V denotes the sample volume. k denotes a geometry dependent factor which is 0.5 for samples with square shaped surface of the ab plane and $k = 0.3$ for samples with an elongated rectangular shaped surface of the ab plane. Equations (7)–(9) are valid under the assumption that there is only a magnetization component parallel to the c-axis direction, i.e., for an azimuthal current flow in the supercon-

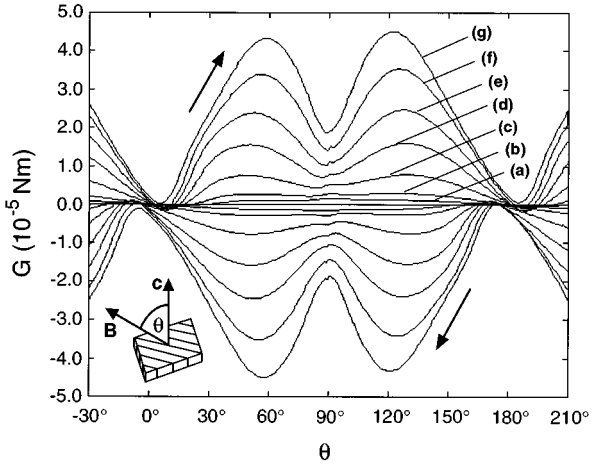

FIG. 1. Experimental torque curves of sample A at $T=77.4$ K for clockwise (lower curves) and counterclockwise rotation (upper curves) for different external magnetic fields H of 40 (a), 80 (b), 160 (c), 240 (d), 320 (e), 400 (f), and 480 kA/m (g). Flux lines were rotating within planes parallel to the twin planes.

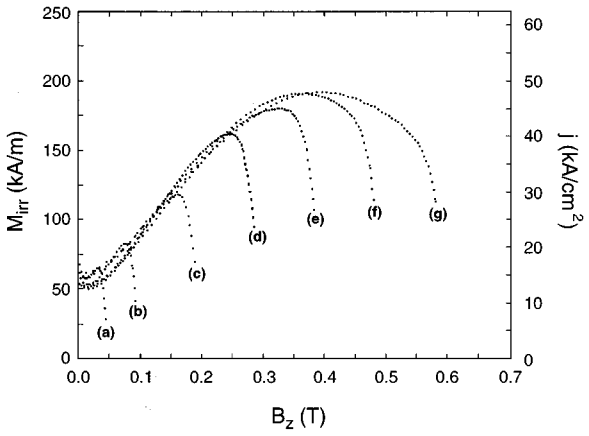

FIG. 2. Irreversible magnetization and current density in dependence on B_z calculated from the data of Fig. 1.

ducting CuO_2 planes. From current density, the pinning force volume density was calculated according to

$$F_p = jB_z . \tag{10}$$

In addition to field rotation experiments, some torque measurements were carried out with time varying magnetic fields and fixed angular orientation of the external magnetic field with respect to the c axis. In these measurements the external magnetic field was swept up and down with field amplitudes up to 7 T. Like in the measurements with rotating magnetic field, a voltage criterion of $E \approx 2.5 \times 10^{-6}$ V/m was achieved in all measurements by choosing an appropriate constant sweep rate of the external magnetic field according to Eq. (7).

For these ''field-loop'' torque measurements a capacitive measurement technique was used to detect the torque signal: The sample was fixed on top of a capacitor plate which was elastically coupled with an opposing capacitor plate by cross springs. The angular orientation of this second plate was fixed in the experimental setup. From the exerted torque a small distortion of the springs and therefore a change of the distance between the opposing plates results. The torque signal was detected by measuring the change of the capacity of these capacitor plates as described in detail elsewhere.[28]

IV. RESULTS AND DISCUSSION

The experimentally observed different magnetization behavior of the different types of samples will be classified in the following in terms of the dimensionality of the most important class of pinning centers in the crystals. We distinguish between collective pinning at randomly distributed point defects (sample A), additional contributions of correlated pinning at twins (samples B and C) and a transitional case where, by changing the external magnetic field direction, a ''lock-in'' transition towards correlated pinning at the twin planes is observed (sample D).

A. Pinning at randomly distributed point pinning centers

Torque curves for crystal A are shown in Fig. 1. This crystal represents the class of samples with only one of the two possible orientations of twin boundaries and samples with only a very low mean twin density. The magnetic field was rotating with constant rotation rate in a plane parallel to the twin planes. Experiments with perpendicular rotational plane, i.e., with the rotating magnetic field cutting the twin planes at $\vartheta_H = 0°$ and 180°, showed no significant deviation from the torque curves of Fig. 1. Therefore pinning in this crystal is not dominated by pinning at twin boundaries (cf. Ref. 29).

Using the torque hysteresis data of Fig. 1 the dependence of the irreversible magnetization $M_{\rm irr}$ and of the current density j on the component of the magnetic induction in c-axis direction $B_z \cong \mu_0 H \cos\theta$ of sample A were calculated for different fixed values of the external magnetic field H according to Eqs. (8) and (9). These data are shown in Fig. 2. The descending branches of the $j(B_z)$ curves, near the maximum values of $B_z \cong \mu_0 H$, can be neglected. They are caused by an inhomogeneous current distribution after reversing the direction of the induction of the azimuthal electric field in the sample. This occurs for the configuration with flux density parallel to the c-axis direction, i.e., for $\theta = 0°$ or 180°. A similar effect can be observed in measurements of magnetization loops with field direction parallel to the c-axis direction after changing from the field increasing branch to the field decreasing branch of the magnetization loop, i.e., close to the maximum field amplitude. This can be explained by the Bean model: Opposing azimuthal currents in an inner and an outer region of the ab planes of the sample superpose resulting in a lower value of the magnetic moment and therefore a lower average current density according to Eq. (9). It should be mentioned here that the current density also may be lowered by the reduced induced electric field in the regime near to $\theta = 0°$ or 180° due to the lowered dH_z/dt according to Eq. (7).

Outside of the just discussed descending branches we get a good scaling of the current density j with B_z for different H and different field orientation ϑ_H (i.e., different vortex orientation θ in the sample). This means that the current density is nearly completely determined by the magnetic

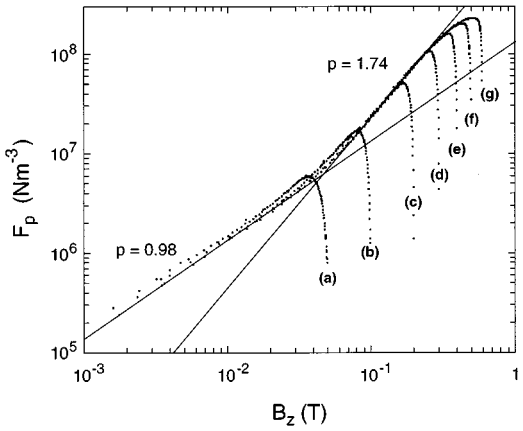

FIG. 3. Pinning force volume density in dependence on B_z determined from the data of Fig. 2.

field component B_z parallel to the c-axis direction. This behavior is well known for the very anisotropic superconductors of the Bi (Ref. 27) and Tl systems (Ref. 30) which may be considered to be two dimensional. The good scaling of the current density with B_z for the different rotational loops in Fig. 2 is due to the anisotropy of the YBCO material. According to the anisotropic GL theory (cf. Ref. 19, p. 1172) current density scales with $B_\epsilon = \epsilon_\theta B$. For the case of YBCO with $\epsilon < 1/7$ (e.g., Ref. 31) the angle-dependent anisotropy parameter $\epsilon_\theta^2 = \epsilon^2(\theta) = \cos^2\theta + \epsilon^2 \sin^2\theta$ can be approximated by $\epsilon_\theta = \cos\theta$ except for a small range around $\theta = 90°$. Because of this good scaling behavior we may substitute B in the equations of the collective pinning theory simply by B_z.

Remarkably, in Fig. 2 current density is increasing with increasing B_z up to 50 kA/cm^2 and is falling down beyond this maximum. This is typical ''fishtail'' behavior as observed in magnetic field sweep measurements for field direction parallel to the c-axis direction. Comparable values of the current density can be reached with melt textured material by optimizing flux pinning by precipitations of impurity phases like Y_2BaCuO_5, platinum, AgO_2, CeO_2, $BaTiO_3$, or other oxides.[32] In this material pinning is assumed to be due to precipitation-matrix interfaces or dislocation networks. In high-quality $YBa_2Cu_3O_{7-\delta}$ thin films current density in general is 2 orders of magnitude higher. The very high current densities in these films, which are 1 order of magnitude lower than the depairing current density, may be understood by the assumption of strong pinning by correlated defects, too. In contrast, taking into account that twin pinning in the present case may be neglected and that precipitations of impurity phases are absent we conclude that pinning in the present crystal is dominated by very densely and randomly distributed weak point pinning centers. Candidates for these pinning centers are point defects on an atomic scale, for instance impurity cations, cation nonstoichiometry and oxygen vacancies. Accordingly, the conditions for collective pinning may be fulfilled.

In order to prove the assumption of a weak random point pinning we analyze the field dependence of our experimental results in terms of the collective pinning theory. For this aim we have plotted the pinning force volume density which is derived from the experimental data of Fig. 2 in bilogarithmic scaling in Fig. 3. Again ignore the rapid drop of the F_p data for different H at high B_z which is caused by the inhomogeneous current distribution in the sample after altering the orientation of the induced electric field in the rotational loops when the maximum value of B_z has been passed. The data of Fig. 3 show a crossover between two power laws of the form $F_p \sim B_z^p$. For very low B_z a linear increase of the pinning force volume density with B_z, i.e., $F_p \sim B_z^{0.98}$, can be observed which is, according to Eq. (10), equivalent to a constant current density independent on B_z. This is characteristic for the regime of single vortex pinning which is expected at low flux densities. It should be pointed out, that for the present measurements with constant rotating magnetic field the repulsive vortex-vortex interaction depends mainly on the distance between flux line kinks in the ab planes and not on the distance between neighboring flux lines. This is in accordance with our assumption that we can substitute B by B_z for our analysis of the experimental data.

For higher flux densities a crossover towards a power law of the form $F_p \sim B_z^{1.74}$ occurs and current density is no longer independent on B_z but shows a characteristic power law behavior of the form $j \sim B_z^{0.74}$, i.e., current density is increasing with B_z. In fact, this power law is predicted for the dependence of current density on flux density in the regime of collective pinning of small flux bundles. In the limit of low depinning temperatures $T \gg T_L^*$ we get from the dependence of T_L^* on $\sqrt{B}$ according to Eq. (2) that the exponential term of Eq. (3) is independent on flux density and that the B dependence of j_{sb} is given by

$$j_{sb} \sim \frac{B}{B_{c2}} \left(1 + \frac{T}{T_L^*(B)}\right)^{1/2} \sim B^{3/4}, \tag{11}$$

resulting in an increase of F_p with B_z of the form $F_p \sim B_z^{7/4}$ as observed in Fig. 3.

This possibility to understand a nonmonotonous behavior of $j(B)$ (i.e., a ''fishtail'' effect) was already pointed out by Feigel'man and Vinokur.[5] The present data prove quantitatively that we deal with the regime of collective pinning of small flux bundles. The ''fishtail'' effect in the present case may be understood due to c_{66} in the preexponential factor in Eq. (4) which is, according to Eq. (1), linear dependent on flux density at low field strengths. The linear increase of the shear modulus c_{66} with B_z is equivalent to an increase of stiffness of the FLL, i.e., a hardening of the FLL. This is in contrast to models, which try to explain the ''fishtail'' increase of j by an improved fit of the FLL at randomly distributed pinning centers due to weakened elastic moduli. An increase of current density due to a hardening of the FLL was discussed for the first time by Vinokur, Kes, and Koshelev.[33] In the framework of the 2D-collective pinning theory they obtained a power-law increase of $j(B_z)$ of the form $j(B_z) \sim B_z^{3/2}$. They attribute this increase of $j(B_z)$ to a suppression of thermal oscillations of the 2D flux lines due to the hardening of the 2D FLL which leads to an enhancement of the strength of the pinning potential. Qualitatively an increase of current density with B_z could be observed in different single-crystalline samples of layered HTS materials as, for instance, $Bi_2Sr_2CaCu_2O_{8+x}$ (Refs. 34 and 35) and $Tl_2Ba_2CaCu_2O_{8+x}$ (Ref. 35) single crystals.

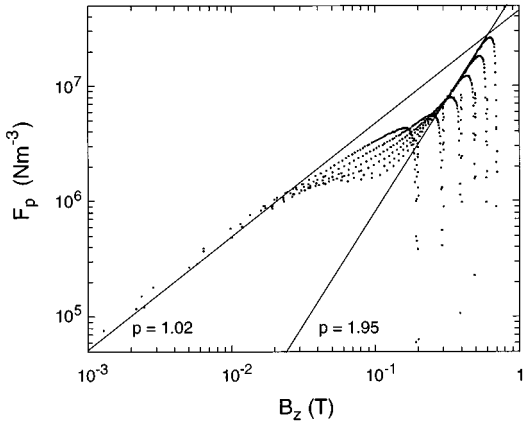

FIG. 4. Pinning force volume density in dependence on B_z for sample B in bilogarithmic representation.

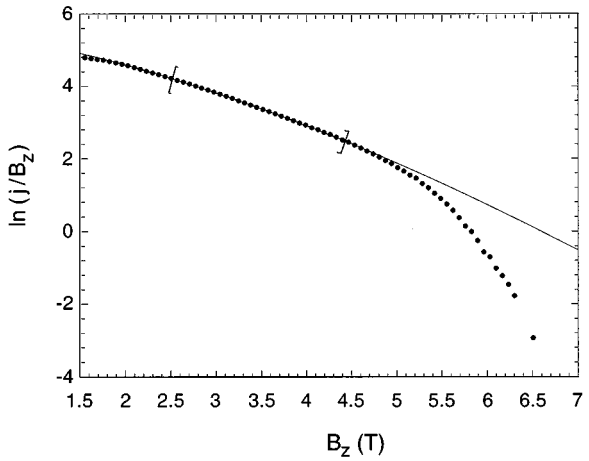

FIG. 5. Nonlinear fit (solid line) in the range between $B_z = 0.5$ T and $B_z = 4.4$ T (indicated by brackets) to the $\ln(j/B_z)$ data of sample C (full dots).

B. Additional contributions of correlated pinning by twins

Experimentally, besides the above-discussed ''fishtail'' effect with $p = 7/4$ a second type of ''fishtail'' effect can be observed which is characterized by a linear increase of the current density with B_z. As shown in Fig. 4 for the $F_p(B_z)$ data calculated from torque magnetometry measurements at 77.4 K for sample B a transition from the single vortex pinning regime with constant current density (i.e., $p = 1.02 \approx 1$) for very low B_z towards a power-law behavior with $p = 1.95 \approx 2$ (i.e., a linear increase of the current density with increasing B_z) occurs. Typical for this class of $YBa_2Cu_3O_{7-\delta}$ single crystals is a twin pattern of ''mosaic''-like structure consisting of twin planes of both of the two possible orientations (110) and (1$\bar{1}$0). As we have seen in the last section for single crystals with only twins of one of the two possible orientations or single crystals with only a very low average twin density (sample type A), pinning is due to weak random point pinning and is not effected by twins. In contrast, for the present case of sample B we suppose that there is a strong twin influence on pinning. It was shown[36] by TEM that boundaries between different twin domains may be regions of large lattice stress which may act as pinning centers being correlated along the c-axis direction.

On the other hand, it is well known from the literature that columnar defects, induced by heavy-ion irradiation, in $YBa_2Cu_3O_{7-\delta}$ thin films[37] [and even in layered HTS compounds as $Bi_2Sr_2CaCu_2O_x$ (cf. Ref. 38)] lead to an enhancement of the in-plane current density for flux-line direction parallel to the direction of the columnar defects. (For the case of layered compounds this is due to a recoupling of 2D vortices in neighboring CuO_2 planes.[39]) In common, as a result of interlayer coupling, a high correlation of pins will result in a stronger pinning in $YBa_2Cu_3O_{7-\delta}$. In analogy twin boundaries will act as correlated pinning centers.

The observed linear increase of current density with B_z, for low B_z, can be understood by means of Eq. (3) if the influence of (i) thermal fluctuations can be neglected (i.e., $T \ll T_L^*$) and (ii) the influence of B_z on the exponent of Eq. (3) is small which means that $\gamma/\gamma_{\max}$ is high (i.e., high correlation of pins). One may expect that $T \ll T_L^*$ is valid due to the stronger pinning at correlated defects. The relation of Eq. (2) for T_L^* was derived for the case of very weak point pinning: The mean elongation of flux lines in an unpinned FLL due to thermal disorder was compared to the range of pinning centers of the order of ξ. The influence of thermal fluctuations on disorder was expected to be high for temperatures higher than the, in this manner approximated, T_L^*.

For stronger pinning due to additional pinning contributions of correlated defects, the approximation Eq. (2) is no longer valid. We suppose that thermal fluctuations of flux lines pinned by randomly distributed point pinning centers are effectively reduced if in addition flux lines are correlated pinned by twin boundaries of both orientations. Only in this case elastic vortex-vortex interactions can reduce the thermal fluctuations of the large fraction of flux lines which are pinned by weak point pinning centers. The reason for this behavior is the suppression of the contribution of the tilt mode to the transverse deformation field by the correlated pinned flux lines.

In the limit of a negligible small contribution of thermal fluctuations to disorder we get from Eq. (3)

$$j_{sb} = \frac{3\sqrt{3}}{32\pi}\, j_0\, \frac{B}{B_{c2}} \exp\left(-\frac{\pi\sqrt{2}}{B_{c2}^{3/2}}\, \frac{\gamma_{\max}}{\gamma}\, B^{3/2} \right). \qquad (12)$$

The same $j(B)$ behavior is also predicted by the theory of Larkin, Marchetti, and Vinokur[16] for the case of correlated twin pinning of a fraction of vortices of the FLL.

To prove our hypothesis of the stronger average correlation of the pinning centers for this class of single crystals we tested the dependence of the exponent of Eq. (12) on B with experimental data from a field-loop torque measurement of sample C. These measurements were performed at $T = 77.4$ K with a constant inclination angle of the external magnetic field with respect to the c-axis direction of $\vartheta_H = 15°$. As demonstrated in Fig. 5, from a nonlinear fit of the experimental data with

$$\ln(j/B) = c_0 - c_1 B^m \qquad (13)$$

in the range between $B_z = 0.5$ T and $B_z = 4.4$ T we obtain a power of $m = 1.499$. This is in excellent agreement with $m = 3/2$ predicted by Eq. (12).

The rapid drop of the data at high $B_z > 5.0T$ is caused by the inhomogeneous current distribution in the sample due to

altering of the direction of the induced electric field after passing the maximum of the external magnetic field of $\mu_0 H = 7\,T$ in our field-loop experiment (cf. the discussion of the rapid drop of data near to the maximum B_z in Figs. 2 and 3 for torque measurements with rotating external magnetic field). Therefore we have omitted these data for our nonlinear fit. For the parameters c_0 and c_1 in Eq. (13) we get from the nonlinear fit in Fig. 5 $c_0 = 5.51$ and $c_1 = 0.326$. Taking into account $B_{c2} \cong 24$ T at $T = 77.4$ K for YBCO we get from Eqs. (12) and (13) a depairing current density of $j_0 \cong 1.15 \times 10^{12}$ A m^{-2} and for the ratio $\gamma_{\max}/\gamma \cong 8.6$. It is interesting to notice that from a nonlinear fit of Eq. (3) to experimental $j(B_z)$ data from field-loop torque measurements of sample A performed under the same conditions ($T = 77.4$ K, $\vartheta_H = 15°$, $E = 2.5 \times 10^{-6}$ V/cm (Refs. 40 and 41) we get nearly the same value for the depairing current density of $j_0 \cong 0.95 \times 10^{12}$ A m^{-2}, a depinning temperature of $T_L^* \cong 260\sqrt{B_z}$ for B_z in T and T_L^* in K, and for the ratio $\gamma_{\max}/\gamma$ we get $\cong 27$. Therefore we have determined for sample A and sample C the same depairing current density and a correlation parameter γ for sample C which is a factor of 3 higher than γ for sample A. This is in good agreement with our hypothesis of a stronger average correlation of pinning in this kind of samples due to an additional contribution of correlated twin pinning.

In general the observed increase of the current density with increasing flux-line density can be explained in the framework of collective pinning of small flux bundles no matter whether there is a remarkable contribution of thermal fluctuations to disorder in the small bundle regime or not. In both cases the increase is related to a hardening of the FLL [i.e., a linear increase of the shear modulus c_{66} in the preexponential factor of Eq. (4) with B for low flux densities as discussed above] and randomly distributed point pinning centers, which have in both cases the main contribution to flux-line pinning. Therefore the suggestion that current increase is a consequence of the suppression of thermal oscillations due to the hardening of the FLL within the small bundle regime is not appropriate for the case of 3D collective pinning in $YBa_2Cu_3O_{7-\delta}$. Otherwise only a $j(B_z) \sim B_z^{3/4}$ power law (cf. Sec. IV A) would be observed but not the linear increase of j with B_z discussed here. The influence of thermal fluctuations of flux lines within the pinning barriers diminishes the current increase from a linear increase $j(B_z) \sim B_z$ towards the $j(B_z) \sim B_z^{3/4}$ power law.

C. ''Lock-in'' transition of correlated twin pinning

The data of samples A, on the one hand, and B and C, on the other hand, represent the typical cases of two different power laws of the ''fishtail'' increase of current density with flux-line density. In comparison, we will report now on an intermediate case which gives further qualitative support to the outlined model. Besides the correlated defects just discussed it has to be assumed that crystal B contains nearly the same order of magnitude of point defects as crystal C. Crystal D to be discussed in the following differs from crystal C in that he shows much lower current densities which is due to a lower concentration of point defects. Accordingly, an interesting transition behavior between pure random point pinning and pinning with additional contributions of correlated pinning is found in crystal D as will be shown below.

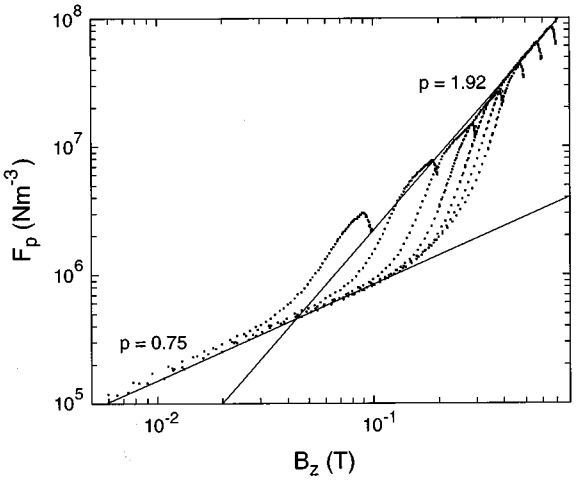

FIG. 6. Pinning force volume density in dependence on B_z of sample D in bilogarithmic representation.

In Fig. 6 the pinning force volume density F_p determined from torque measurements with rotating external magnetic field of sample D at a temperature of $T = 77.4$ K is shown in dependence on the flux density component B_z in bilogarithmic representation.

Here we can observe a crossover from a power-law behavior at very low flux densities of the form $F_p \sim B_z^{3/4}$ towards a ''fishtail'' behavior $F_p \sim B_z^2$, i.e., a linear increase of j with B_z for stronger fields. Current density in dependence on B_z is shown in Fig. 7. Note that the current density is 1 order of magnitude lower than for the same type of measurements for sample A, as shown in Fig. 2, especially at low B_z in the $F_p \sim B_z^{3/4}$ regime. A good scaling for this regime as well for the linear ''fishtail'' increase of j with B_z, which is indicated by the solid line to the data points as a guide for the eye, can be observed.

In the framework of collective pinning theory a low current density, i.e., very weak pinning, corresponds with a large correlation volume, i.e., a large size of the flux-line bundle. Indeed the collective pinning theory of large flux bundles gives a quantitative explanation of the scaling behavior of j with B_z of the form $j(B_z) \sim B_z^{-1/4}$. If the contribution of thermal oscillations of flux lines to disorder is large, i.e., if T_L^* according to Eq. (2) is much lower than the measurement temperature of $T = 77.4$ K, we have $(1 + T/T_L^*)^{-11/2} \sim B^{11/4}$. In this case Eq. (5) predicts a power-law behavior of the form $j_{lb} \sim B_z^{-1/4}$.

For intermediate B_z the scaling of the $j(B_z)$ curves for different values of the external field strength H in Fig. 7 is quite bad. We have determined the points of inflection in the transitional branches between the two regimes in the $j(B_z)$ curves of Fig. 7. The inset in Fig. 7 shows the angle θ_{ip} of field inclination of the external magnetic field with respect to the c-axis direction for these points of inflection in dependence on H. For different external fields up to 0.8 T we find that θ_{ip} is nearly independent on H. Therefore we conclude that the transition between the two regimes of collective pinning in Fig. 7 is due to the change of flux-line orientation in the crystal.

The behavior observed in Fig. 7 can be explained in terms of a transition from weak random point pinning of all flux

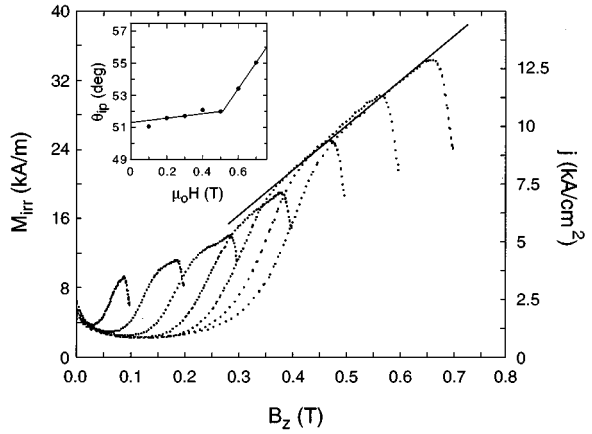

FIG. 7. Scaling behavior of $j(B_z)$ of sample D. Inset: Angle θ_{ip} of the inflection point of the $j(B_z)$ curves for different values of H. Solid lines are guides for the eye (cf. text).

lines at defects in the superconducting CuO_2 planes towards the ''lock-in'' state, i.e., the state with a fraction of flux-line segments pinned aligned within the twin planes. This transition depends mainly on the flux-line orientation, which is in accordance with the observations of the inset of Fig. 7. We may interpret θ_{ip} as a ''lock-in'' angle, which separates the regime of weak random point pinning of the whole FLL from the regime with contributions of correlated pinning at twins. The fraction of correlated pinned flux lines damps the thermal oscillations of the neighbored vortices and therefore avoids the thermally smearing out of the potential of the point pinning centers. The rapid increase of current density, which can be observed in Fig. 7 for different values of H before achieving the ''fishtail'' regime is due to this suppression of the thermally smearing out of the point pinning centers. As we can see in the inset in Fig. 7 for low external fields $\mu_0 H$ below 0.5 T we find only a very weak dependence of θ_{ip} on flux density and we obtained a nearly constant value of $\theta_{ip} \approx 52°$. For fields above 0.5 T we find a very smooth increase of θ_{ip} with increasing $\mu_0 H$. This is due to the enhanced stiffness of the 3D FLL, which hinders the ''lock-in'' of flux lines into the twin planes and shifts θ_{ip} slightly towards 90°.

V. CONCLUSIONS

In this paper we have reported on the observation of several transitions between different regimes of single vortex pinning and collective flux-line pinning in $YBa_2Cu_3O_{7-\delta}$ single crystals. By investigation of single crystals of different microstructure we have separated the effects of two basic types of pinning centers, random point pinning and correlated pinning due to twin boundaries, on the collective pinning of flux lines. We have shown that the so-called ''fishtail'' effect can be explained as an increase of current density $j(B_z)$ with increasing B_z within the regime of collective pinning of small flux bundles at low field strength related to a hardening of the FLL. For weak random point pinning there is a remarkable contribution of thermal fluctuations to disorder at temperatures of 77.4 K which leads to a power-law behavior $j \sim B_z^{3/4}$ of the current increasing part of the $j(B_z)$ curve. For samples with a ''mosaic'' twin structure, i.e., having a dense network of twin planes of both orientations perpendicular to each other, current increase is linear $j \sim B_z$ in the ''fishtail''-shaped $j(B_z)$ curve. It was shown that this behavior can be attributed to a reduced influence of thermal fluctuations in the regime of small flux bundles. In both types of microstructure the increase of j at low B may be understood in terms of an increase of the shear modulus c_{66}. The effect of increased thermal oscillations in the case of random point disorder in comparison to correlated disorder is a depression of ''fishtail'' increase from linear in the latter case to a 3/4 power law in the first case. The measured field dependence of current density may be quantitatively well interpreted in the frame of a collective pinning theory if known values of upper critical field and depairing current density are used. For the only unknown parameter γ_{max}/γ, i.e., relative pinning strength, reasonable values for both kinds of microstructure are found.

The suggestion that contributions of correlated pinning at twin boundaries of both orientations, in addition to random point pinning, reduce the thermal fluctuations of the FLL is strongly supported by the observation of a ''lock-in'' transition in $YBa_2Cu_3O_{7-\delta}$ single crystals with low current densities: By approaching the vortex orientation parallel to the c-axis direction a crossover, from collective pinning of large flux bundles at randomly distributed weak point pinning centers, which is highly affected by thermal fluctuations, towards a regime of collective pinning of small flux bundles, where thermal fluctuations can be neglected and average correlation of pins is high, occurs. The stronger average correlation of the elementary pinning barriers in these samples can be explained by the ''lock in'' of a fraction of flux lines in the flux bundles into the twin planes. These correlated pinned flux lines drastically reduce the tilt deformations of thermal oscillations of the remaining flux lines. As a consequence thermally smearing out of the point pinning barriers is suppressed, pinning and therefore current density is enhanced and a reduced correlation volume is achieved.

Since orthorhombicity of $YBa_2Cu_3O_{7-\delta}$ depends on the oxygen content and oxygen ordering, and the formation of a dense mosaic twin pattern is related to orthorhombicity, correlated pinning of flux lines at twin boundaries can be influenced by annealing conditions.

Two ''fishtail'' bumps in magnetization curves[42] can be observed for the case that the average distance between the twins is high. In this case the reduction of thermal oscillations can only be achieved at high flux densities. Then a ''fishtail'' bump with $j \sim B_z^{3/4}$ is followed by a ''fishtail'' bump with a linear increase of j with B_z.

The reason why ''fishtail''-shaped magnetization curves cannot be observed for $YBa_2Cu_3O_{7-\delta}$ thin films is caused by the high current densities resulting from the dense distribution of very strong pinning centers in those films. Accordingly single vortex pinning occurs in these samples in a large field range.

In conclusion, it was shown that most essential features of the field dependence of current density of YBCO single crystals at 77.4 K may be consistently described by the collective pinning theory taking into account typical microstructure properties of that crystals.

ACKNOWLEDGMENTS

The authors greatly appreciate the opportunity to perform a part of the measurements in the group of Professor R. Griessen at the Laboratory of Solid State Physics of the Free University of Amsterdam. They thank A. Erb for sample preparation, T. Klupsch for valuable discussions, and M. Zeisberger for ac-susceptibility measurements. This work was supported by the BMBF under Contract No. 13N6100.

[1] A. I. Larkin and Yu. N. Ovchinnikov, J. Low Temp. Phys. **34**, 409 (1979).
[2] P. H. Kes and C. C. Tsuei, Phys. Rev. Lett. **47**, 1980 (1981).
[3] K. Sugawara, K. Yokota, N. Takei, Y. Tanokura, and T. Sekine, J. Low Temp. Phys. **95**, 645 (1994).
[4] R. Wördenweber and P. H. Kes, Cryogenics **29**, 321 (1989).
[5] M. V. Feigel'man and V. M. Vinokur, Phys. Rev. B **41**, 8986 (1990).
[6] M. Daeumling, J. M. Seuntjens, and D. C. Larbalestier, Nature **346**, 332 (1990).
[7] L. Klein, E. R. Yacoby, Y. Yeshurun, R. Erb, G. Müller-Voigt, V. Breit, and H. Wühl, Phys. Rev. B **49**, 4403 (1994).
[8] M. A. Angadi, Z. X. Shen, A. D. Caplin, D. G. McCartney, L. Leonyuk, A. A. Zhukov, and G. Emelchenko, Supercond. Sci. Technol. **5**, 165 (1992).
[9] A. A. Zhukov, H. Küpfer, G. Perkins, L. F. Cohen, A. D. Caplin, S. A. Klestov, H. Claus, V. I. Voronkova, T. Wolf, and H. Wühl, Phys. Rev. B **51**, 12 704 (1995).
[10] T. Tamegai, Y. Iye, I. Oguro, and K. Kishio, Physica (Amsterdam) C **213**, 33 (1993).
[11] Y. Yeshurun, N. Bontemps, L. Burlachkov, and A. Kapitulnik, Phys. Rev. B **49**, 1548 (1994).
[12] L. Krusin-Elbaum, L. Civale, V. M. Vinokur, and F. Holtzberg, Phys. Rev. Lett. **69**, 2280 (1992).
[13] R. Hergt, R. Hiergeist, A. Erb, J. Less-Common Alloys Compd. **195**, 431 (1993).
[14] H. Küpfer, S. N. Gordeev, W. Jahn, R. Kresse, R. Meier-Hirmer, T. Wolf, A. A. Zhukov, K. Salama, and D. Lee, Phys. Rev. B **50**, 7016 (1994).
[15] W. K. Kwok, J. A. Fendrich, C. J. van der Beek, and G. W. Crabtree, Phys. Rev. Lett. **73**, 2614 (1994).
[16] A. I. Larkin, M. C. Marchetti, and V. M. Vinokur, Phys. Rev. Lett. **75**, 2992 (1995).
[17] E. H. Brandt, J. Low Temp. Phys. **26**, 735 (1977).
[18] V. M. Vinokur, M. V. Feigel'man, V. B. Geshkenbein, and A. I. Larkin, Phys. Rev. Lett. **65**, 259 (1990).
[19] G. Blatter, M. V. Feigel'man, V. B. Geshkenbein, A. I. Larkin, and V. M. Vinokur, Rev. Mod. Phys. **66**, 1125 (1994).
[20] See e.g., H. G. Schnack, R. Griessen, J. G. Lensink, and M. H. Wen, Phys. Rev. B **48**, 13 178 (1993).
[21] V. V. Moshchalkov, V. V. Metlushko, G. Güntherodt, I. N. Goncharov, A. Yu. Didyk, and Y. Bruynseraede, Phys. Rev. B **50**, 639 (1994).
[22] V. V. Metlushko, G. Güntherodt, V. V. Moshchalkov, and Y. Bruynseraede, Europhys. Lett. **26**, 371 (1994).
[23] A. Erb, T. Biernath, and G. Müller-Vogt, J. Cryst. Growth **132**, 389 (1993).
[24] H. Claus, M. Braun, A. Erb, K. Röhberg, B. Runtsch, H. Wühl, G. Bräuchle, P. Scheib, G. Müller-Vogt, and H. V. Löhneysen, Physica (Amsterdam) C **198**, 42 (1992).
[25] M. Zeisberger (private communication).
[26] M. Schmelz (unpublished).
[27] R. Hergt, R. Hiergeist, J. Taubert, H. W. Neumüller, and G. Ries, Phys. Rev. B **47**, 5405 (1993).
[28] R. Griessen, C. F. J. Flipse, C. W. Hagen, J. Lensink, B. Dam, G. M. Stollman, J. Less-Common Met. **151**, 39 (1989); See as well M. Qvarford, K. Heeck, J. G. Lensink, R. J. Wijngaarden, and R. Griessen, Rev. Sci. Instrum. **63**, 5726 (1992).
[29] R. Hergt, W. Andrä, R. Hiergeist, and J. Taubert, Phys. Status Solidi A **129**, 237 (1992).
[30] W. Andrä, R. Hergt, R. Hiergeist, J. Taubert, M. Zeisberger, K. Winzer, J. Bernhard, and K. F. Renk, Physica (Amsterdam) C **213**, 471 (1993).
[31] D. E. Farrell, J. P. Rice, D. M. Ginsberg, and J. Z. Liu, Phys. Rev. Lett. **64**, 1573 (1990); B. Janossy, R. Hergt, and L. Fruchter, Physica (Amsterdam) C **170**, 22 (1990).
[32] M. Murakami, S. Gotoh, H. Fujimoto, K. Yamaguchi, N. Koshizuka, and S. Tanaka, Supercond. Sci. Technol. **4**, 43 (1991); *Melt Processed High-Temperature Superconductors*, edited by M. Murakami (World Scientific, Singapore, 1992).
[33] V. M. Vinokur, P. H. Kes, and A. E. Koshelev, Physica (Amsterdam) C **168**, 29 (1990).
[34] G. Yang, P. Shang, S. D. Suttont, I. P. Jones, J. S. Abell, and C. E. Gough, Phys. Rev. B **48**, 4045 (1993).
[35] T. Tamegai, S. Ooi, T. Shibauchi, Y. Matsushita, M. Hasegawa, H. Takei, M. Ichihara, and K. Suzuki, Physica (Amsterdam) C **235-240**, 2817 (1994).
[36] Y. Zhu, M. Suenaga, and J. Tafto, Philos. Mag. A **67**, 1057 (1993).
[37] B. Holzapfel, G. Kreiselmeyer, M. Kraus, S. Bouffard, S. Klaumünzer, L. Schultz, and G. Saemann-Ischenko, J. Less-Common Alloys Compd. **195**, 411 (1993).
[38] M. Konczykowski, N. Chikumoto, V. M. Vinokur, and M. V. Feigel'man, Phys. Rev. B **51**, 3957 (1995).
[39] A. E. Koshelev, P. Le. Doussal, and V. M. Vinokur, Phys. Rev. B **53**, R8855 (1996).
[40] R. Hiergeist, Ph.D. thesis, Universität Jena, 1995.
[41] R. Hiergeist, R. Hergt, A. Erb, H. G. Schnack, and R. Griessen, Physica (Amsterdam) C **235-240**, 2743 (1994).
[42] R. Hiergeist (unpublished).